analytical chemistry

Article

pubs.acs.org/ac

Sourcing of Copper and Lead within Red Inclusions from Trinitite Postdetonation Material

Elizabeth C. Koeman,*[,†] Antonio Simonetti,[†] and Peter C. Burns[†,‡]

[†]Department of Civil and Environmental Engineering and Earth Sciences and [‡]Department of Chemistry and Biochemistry, University of Notre Dame, Notre Dame, Indiana 46556, United States

Supporting Information

ABSTRACT: Historical postdetonation materials resulting from nuclear testing can be used to develop methodologies for source attribution, in particular if the chemical and isotopic signatures of the device are public domain. The samples analyzed in this study are from the world's first nuclear bomb explosion in 1945, the Trinity Test, and produced the postdetonation material "Trinitite". The latter is a glassy material that resulted from the melting of the natural sand present at ground zero (Alamogordo, NM) and incorporated components of the device. Chemical and isotopic (e.g., Pu) information on the device is declassified and, therefore, methodologies for fingerprinting fuel and other device components can be verified. One type of Trinitite contains red inclusions that are characterized by high concentrations of Pb (between 438 and 26,631 μg/g) and Cu (between 404 and 22,280 μg/g) that are in general positively correlated. Pb isotope compositions for the red inclusion areas exhibit a large variation and indicate mixing between Pb from at least 3 different sources: 1- natural geological background (arkosic sand) present at ground zero; 2- anthropogenic component from the device; and 3- industrial Cu used for wiring in the device. Based on the Pb isotope ratios for the red inclusions within Trinitite, it is likely that the anthropogenic Pb derives from Buchans Mine (Newfoundland, Canada), which is in agreement with a previous investigation. Products of industrial Cu manufacturing (e.g., pennies) were analyzed for their trace element abundances and Pb isotope compositions; these suggest that Cu employed within the device's wiring was derived from two Cu ore deposits within the USA.

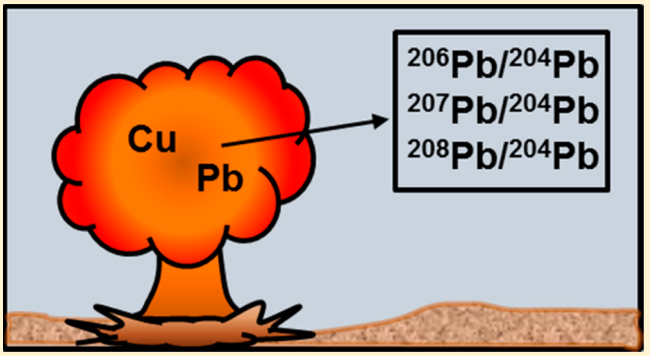

Postdetonation materials (PDMs) play a crucial role in the field of nuclear forensics since they can contain device components originating from a nuclear explosion and may be the only route that can lead to source attribution. Chemical and isotopic compositions of both device components and fuel are needed for accurate determination of their origin in PDMs.[1−5] The methodologies developed in the latter studies used readily accessible PDMs known as "Trinitite", material produced subsequent to the world's first nuclear bomb detonation. Trinitite is ideal to study because the device components are declassified, and therefore results obtained during forensic investigations can be verified.

The Pu-implosion device employed in the Trinity test was nicknamed "Gadget" and was detonated at 5:29:45 a.m. on July 16, 1945 at White Sands Missile Range near Alamogordo, NM. The 6 kg mass of Pu consisted predominantly of ^{239}Pu (^{240}Pu/^{239}Pu ~0.013) and was surrounded by a tamper consisting of natural uranium.[1−5] The device also contained Cu wiring, aluminum shells, and framing and was detonated at the top of a 30 m steel tower. The explosion of the device melted all of its components along with the top layer (~1−2 cm) of the natural desert sand contained within the blast area, which resulted in the production of Trinitite. The minerals present within the arkosic sand at ground zero include quartz, feldspars (microcline and albite plagioclase), calcite, gypsum, halite, hornblende, olivine, magnetite, ilmentite, augite, zircon, monazite, and clay minerals kaolinite and illite.[1,6]

Red inclusions within Trinitite have been referenced in previous studies[3,6−9] but have not been investigated in great detail for their trace element and isotope compositions. These inclusions are somewhat rare and are interpreted to originate from the Cu wiring of the device. Scanning electron microscopy (SEM) and energy dispersive spectroscopy (EDS) analysis confirmed that the red areas within "green" Trinitite were enriched in Cu and Pb abundances. Bellucci and Simonetti (2012)[9] observed Pb (as an oxide) and Cu on the surfaces of Trinitite. Pb isotope compositions of the predominant "green" Trinitite have been used in a previous study to determine the provenance of the anthropogenic Pb contained within the different components of the nuclear device.[3]

Lead has 4 isotopes: ^{204}Pb, ^{206}Pb, ^{207}Pb, and ^{208}Pb, and the latter three result from the decay of long-lived isotopes ^{238}U, ^{235}U, and ^{232}Th, respectively (in addition to the primordial Pb

Received: February 19, 2015
Accepted: April 23, 2015
Published: April 23, 2015

DOI: 10.1021/acs.analchem.5b00696
Anal. Chem. 2015, 87, 5380−5386

abundances present at the time of solar system formation); in contrast, ^{204}Pb is the only nonradiogenic isotope of Pb, and its abundance is constant in nature. Therefore, the present-day Pb isotope composition of any geological or anthropogenic sample is a function of its Pb isotope composition at the time of its formation, the Th−U−Pb ratios, and its age. Hence, the natural variation of Pb isotope compositions in rocks and Pb-bearing minerals (e.g., galena- PbS) can be used as an effective isotopic fingerprint tool. Pb extracted from ore deposits has been exploited by civilizations over thousands of years for a variety of purposes (metallurgical, medicinal, and industrial), therefore, making Pb one of the most heavily utilized metals during human history. Consequently, the Pb isotopic signatures of major industrial sources of Pb worldwide have been sufficiently characterized so as to permit source apportionment calculations with some degree of certainty.[10]

The exact use of the industrial Pb present within the Trinity device is not known since it was not documented; however, Pb bricks could have been used for shielding purposes.[3,8] Also, while the Trinity device contained a U tamper, Pb could be employed as a tamper in a nuclear device.[3] Therefore, developing a methodology to source the origin of Pb is of importance to nuclear forensics. Based on the highly variable Pb isotope ratios recorded for "green" Trinitite, Bellucci et al.[3] reported an estimated Pb isotope composition for the industrial Pb contained within the Trinity device.

This study focuses exclusively on the Pb- and Cu-rich red inclusion areas of Trinitite with the intent of providing a better estimate of the Pb isotope composition for the materials used in the Trinity device. Moreover, due to the intimate association between Pb and Cu abundances in the red inclusions of Trinitite, this investigation also attempts to source the provenance of the industrial Cu present within Trinitite. Trace element signatures within Cu have been used in provenance studies for artifacts of Native American origin,[11] which attempt to trace the Cu back to their geologic source.[12,13] Rapp et al.[11] investigated the trace element signature of 75 Cu samples taken from different ores in North America and demonstrated that these may be used to source Cu artifacts. Pb isotope ratios from Cu artifacts have also been used in provenance studies,[14] as well as tracing atmospheric pollution originating from Cu smelting.[15] In order to determine the source of Cu used in the Trinity device, two samples of manufactured (industrial) Cu produced from the Bingham Mine (Utah) and Keweenaw native Cu deposit (Upper Peninsula, Michigan), both of which were in operation and large producers of Cu in the US in the beginning of the 20th century,[16,17] were analyzed for their Pb isotope compositions; these are then compared to the Pb isotope ratios of Trinitite. For comparative purposes, the Pb isotope compositions of two US pennies are also reported: one produced in 1946 (shortly after the Trinity test) and the other in 2013.

■ ANALYTICAL METHODS

Samples. Trinitite samples were purchased from the Mineralogical Research Corporation (www.minresco.com). Out of 70 samples, 3 were classified as having red inclusions and are the focus of this study (Figure 1). Samples were sectioned and polished to a thickness of ∼100 μm. Samples of industrial Cu (Figure 2) include the following: 1- a US penny produced in 1946; 2- a US penny produced in 2013; 3- a Cu nugget from Keweenaw Peninsula (MI); and 4- a Cu-based souvenir manufactured from the Bingham Mine (UT).

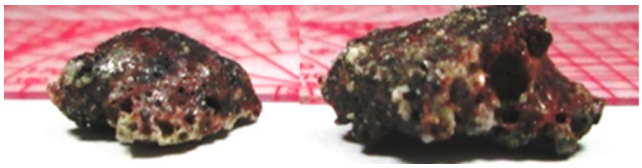

Figure 1. Photo of red Trinitite samples investigated here.

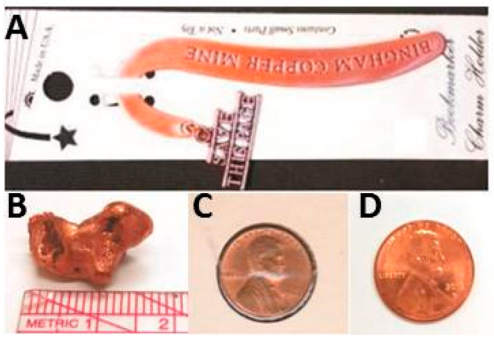

Figure 2. Bingham, UT Cu souvenir (A), Cu nugget from Keweenaw Peninsula, MI (B), 1946 penny (C), and 2013 penny (D) investigated here for trace element abundances and Pb isotope ratios.

Imaging. Maps of Trinitite thin sections were constructed using a petrographic microscope equipped with a digital camera. Photos were taken in plane polarized light and stitched together with the use of Adobe Photoshop (Figure 3A). Back scatter electron (BSE) images (Figure 3B) were taken with an EVO 50 LEO Environmental Scanning Electron Microscope (SEM, Carl Zeiss) at the Notre Dame Integrated Imaging Facility. An EDAX Orbis Micro Energy Dispersive X-ray Fluorescence (Micro-XRF) instrument was used to collect chemical maps of thin sections using an X-ray aperture size of 30 μm, dwell time of 100 ms, and voltage of 50 kV. Resolution for maps is 512 × 480 pixels (Figure 3).

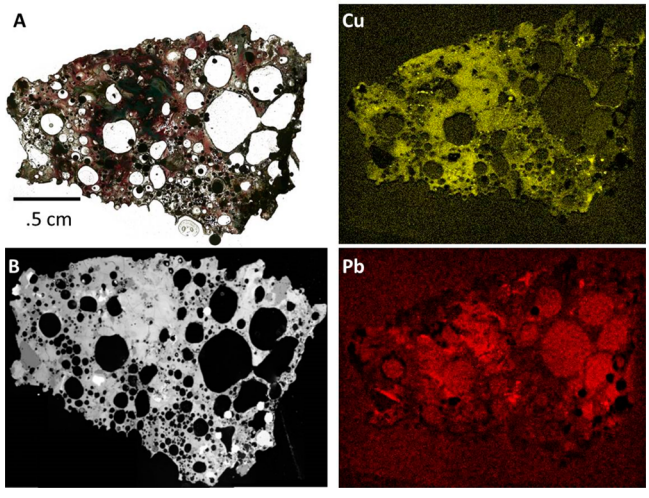

Figure 3. Plane-polarized image of red Trinitite sample (A) with corresponding backscattered image (B). Major element chemical maps obtained by μ-XRF are labeled by element.

Electron Microprobe Analysis (EMPA). Major element determinations in red inclusion areas were conducted at the

DOI: 10.1021/acs.analchem.5b00696
Anal. Chem. 2015, 87, 5380−5386

University of Chicago with a Cameca SX-50 electron microprobe. An accelerating voltage of 15kV was used, along with a beam size of 15 μm and a beam current of 35 nA. The following well-characterized standards were used for calibration purposes: olivine (Fe, Mg, Mn), albite (Na), anorthite (Ca, Al), asbestos (Si), microcline (K), and rutile (Ti). Uncertainties (2σ mean) are based on counting statistics and are $\leq$2% for SiO_2, Al_2O_3, and CaO; $\leq$5% for FeO, Na_2O, and K_2O; and $\leq$10% for MnO, MgO, and TiO_2.

Solution Mode-ICPMS Analyses. Bulk samples of industrial Cu and Trinitite were analyzed for their trace elements abundances using solution mode inductively coupled plasma mass spectrometry (ICPMS). Cu samples were cut into small pieces weighing between ~0.08 and ~0.1 g and were subsequently washed in Savillex Teflon beakers with ultrapure water (18 MΩ) and double-distilled (2D) 5% HNO_3 while in an ultrasonic bath (for 45 min). The Cu pieces were then dissolved in 2D concentrated HNO_3 acid, dried down overnight, and diluted with 5% HNO_3 (~100 mL). Trinitite samples were digested using a mixture of concentrated HF:HNO_3 acid (4:1 ratio) in closed 15 mL Savillex Teflon beakers on a hot plate at ~120 °C for 48 h. The samples were then dried down and fluxed twice in concentrated HNO_3 acid within capped Teflon beakers for a period of 24 h (each cycle). These were then dried down, redissolved in concentrated nitric acid, and subsequently diluted to a final volume of 100 mL with ultrapure (18 MΩ) water. Trace element abundances were determined using a standard/spike addition method.[18]

LA-(MC)-ICPMS. *In situ* laser ablation (LA)-ICPMS analyses for trace element determinations were conducted with a New Wave Research UP-213 laser ablation unit coupled to a ThermoFinnegan Element2 sector-field high resolution (HR)-ICPMS. Background ion signals were collected for 60 s with the laser on and shuttered, followed by 60 s of ion signal collection. A "standard-sample" bracketing technique was employed with analyses of the NIST SRM 612 international standard glass wafer to monitor for instrumental drift (protocol adopted from Chen and Simonetti[19]). Instrument configuration, settings, dwell times, and a list of all isotopes collected are listed in the Supporting Information. Due to the high ion signals of Pb and Cu, analog detection mode was employed.

In situ Pb isotope ratios obtained using petrographic thin sections were determined using a Nu Plasma II multicollector (MC)-ICPMS coupled to an ESI-NWR193 excimer laser system. Instrument settings and gas flows are listed in the Supporting Information. Background ion signals were taken for 45 s with the laser on (shuttered), and Pb ion signals were collected using five Faraday cups for 40−80 s. The ^{202}Hg ion signal was also collected and used to correct for the isobaric interference of ^{204}Hg on ^{204}Pb. A "standard-sample" bracketing technique was also used with the NIST SRM 612 glass wafer as the external calibration standard. Repeated measurements (n = 19; see the Supporting Information) of NIST SRM 612 yielded average values and associated (2σ) standard deviations as follows: ^{206}Pb/^{204}Pb = 17.10 ± 0.25, ^{207}Pb/^{204}Pb = 15.55 ± 0.21, ^{208}Pb/^{204}Pb = 37.20 ± 0.57. Instrumental mass bias was corrected using the exponential law with NIST SRM 612 values from Baker et al.[20]

The bulk Cu samples investigated for their trace element concentrations were also characterized for their Pb isotope ratios in solution mode MC-ICPMS subsequent sample digestion and ion exchange chromatography. Sample aliquots weighing between 0.05 and 0.15 g were washed twice with ultrapure water (18 MΩ) in an ultrasonic bath for 45 min. When dried, samples were redissolved in 2 mL of 2D HNO_3 for 24 h. The solution was dried overnight and then fluxed with 2 mL of 0.8N 2D (Seastar) HBr for 24 h and last dried down. The Pb separation technique followed that from Manhès et al.,[21] and a brief description of the method is provided here. Columns were made by loading ~20 μL of purified ("lead-free") AG1-X8 resin (75−150 mesh) into a polypropylene tube fitted with a polystyrene frit. The resin bed volume was cleaned twice with 0.15 mL of ultrapure (18 MΩ) H_20 and then conditioned with 0.15 mL of 0.8 N 2D HBr. The sample solution is loaded with 0.6 mL of 0.8 N 2D HBr, washed twice with 0.15 mL of 0.8 N 2D HBr, and last eluted with 0.7 mL of 6 N 2D HCl acid. The collected Pb is dried down, and the ion exchange procedure is performed a second time with new resin in order to further purify the Pb aliquot. Subsequent to the second elution procedure, the Pb aliquot is dried down and redissolved in 2% HNO_3 for solution mode-MC-ICPMS analysis.

The procedure for analyzing the sample solutions for their Pb isotope compositions followed that of Simonetti et al.[15] The Pb aliquot is spiked with a NIST SRM 997 Thallium standard solution (2.5 ppb). Pb and Tl isotopes and ^{202}Hg were measured using seven Faraday cups on the Nu Plasma II MC-ICPMS. The ^{205}Tl/^{203}Tl is measured for monitoring the instrumental mass bias (exponential law; ^{205}Tl/^{203}Tl = 2.3887), and ^{202}Hg was recorded for the ^{204}Hg interference correction on ^{204}Pb. Prior to sample introduction, a baseline measurement of the gas and acid blank ("on-peak-zero") was conducted for 30 s. Data acquisition involved 2 blocks of 25 scans (each scan was 10 s). A 25 ppb solution of the NIST SRM 981 Pb standard (spiked with 6 ppb NIST SRM 997 Tl standard) was also analyzed periodically throughout the analytical session. Repeated measurements (n = 4; see the Supporting Information) of the NIST SRM 981 + Tl standard solution yielded average values and associated (2σ) standard deviations as follows: ^{206}Pb/^{204}Pb = 16.935 ± 0.003, ^{207}Pb/^{204}Pb = 15.488 ± 0.002, ^{208}Pb/^{204}Pb = 36.686 ± 0.008.

RESULTS

Within the red inclusion areas, the larger (cm) scale distribution of Pb, Cu (device-related) and other elements (Si, Ca, K, Al) prominent in the natural sand were delineated by μ-XRF (Figure 3). Quantitative assessment of the Pb abundances at higher spatial resolution (10 s of micron scale) within the red areas by LA-ICPMS indicates concentrations between ~500 and ~27,000 μg/g (e.g., Figure 4; see the Supporting Information). This is extremely high when compared to the Pb concentration of ~40 μg/g in the bulk sand (geological background) at the Trinity Site as well as the maximum value of "green" Trinitite (~1735 μg/g).[22] Figure 4 demonstrates the variability of both the Pb and Cu concentrations in the red areas of Trinitite at the micron scale. Cu is also found at high concentrations of between ~400 and ~23,000 μg/g (Figure 4; see the Supporting Information) within the red areas and also is significantly enriched compared to the bulk sand (~26 μg/g) and maximum "green" Trinitite (~312 μg/g).[22] Bellucci et al.[22] concluded that the abundances of Co, Cr, Cu, and Pb in Trinitite are higher in samples that originate >74 m away from ground zero (GZ). Interestingly, both samples Red A and B are interpreted to have formed >74 m from GZ because they both lack ^{152}Eu activity.[2] Based on the calculations from Bellucci et al. (2013),[2] the ^{152}Eu activity for

DOI: 10.1021/acs.analchem.5b00696
Anal. Chem. 2015, 87, 5380−5386

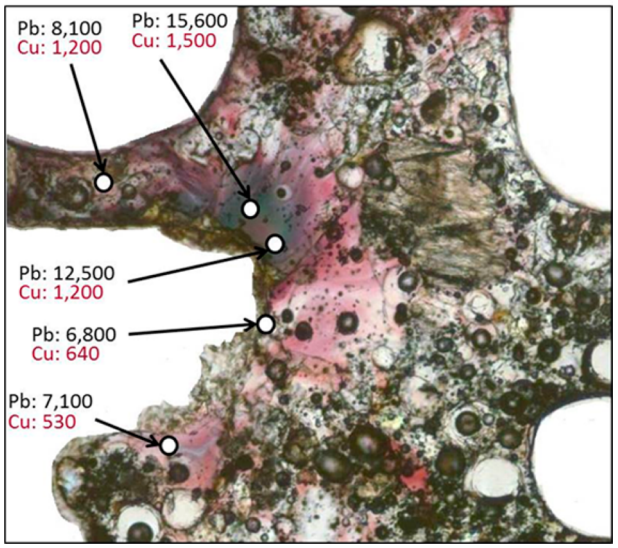

Figure 4. Photo of an area from a red Trinitite thin section (field of view = 2.5 mm). Arrows point to locations of *in situ* LA-ICPMS analysis with the recorded Pb and Cu concentrations in μg/g.

sample 4A 9.86 corresponds to a distance of ~69 m from GZ. The degree of enrichment is dependent on their respective condensation temperatures, which decrease in the following order: Co, Cr, Cu, and Pb. Of interest, red inclusion Trinitite samples A and B contain higher Cu and lower Pb abundances compared to those for sample 4A 9.86 (Figure 5; see the Supporting Information). Figure 5 indicates that the concentrations of Co, Ni, Cu, and Pb are more homogeneous in sample 4A 9.86 compared to those for red Trinitite samples A and B. Moreover, Pb and Cu abundances do not correlate with those for elements (e.g., Si, Ca, K, Al) derived predominantly from the minerals in the natural sand found at ground zero (not shown).

The industrial samples of Cu are characterized by low abundances of metals (e.g., Ni, Co, and Cr) and incompatible (lithophile) elements (e.g., rare Earth elements), which are present below their respective detection limits determined during ICPMS analysis. One notable exception is the relatively high concentration of Zn (287 μg/g) for the Cu sample from the Bingham mine (see the Supporting Information).

Figure 6 illustrates all of the Pb isotope results for "normal" Trinitite glass (from Bellucci et al.[3]) and red inclusion areas of Trinitite from this study. Pb isotope ratios within Trinitite glass define a large range of values (e.g., $^{206}Pb/^{204}Pb$ = 17.08–19.04; Figure 6). In Pb–Pb isotope diagrams, mixing between distinct components yields linear trends (Figure 6). Thus, Bellucci et al.[3] attributed the large (total) range of Pb isotopic ratios recorded by Trinitite glass to mixing between various mineral phases present within the arkosic sand at ground zero. In contrast, the new Pb isotope analyses for red areas of Trinitite reported here (see the Supporting Information) yield a narrower range of Pb isotope ratios (e.g., $^{206}Pb/^{204}Pb$ = 17.20–18.30; Figure 6). However, there is a lack of correlation between the high abundances of Cu and their respective Pb isotope ratios for the samples of red Trinitite investigated here (e.g., Figure 7). The Pb isotope ratios (and associated uncertainties) of the industrial Cu samples examined in this study are listed in the Supporting Information. These values are plotted along with the Pb isotope ratios of red Trinitite and feldspar in Figure 8. Zn and Cu abundances recorded in red

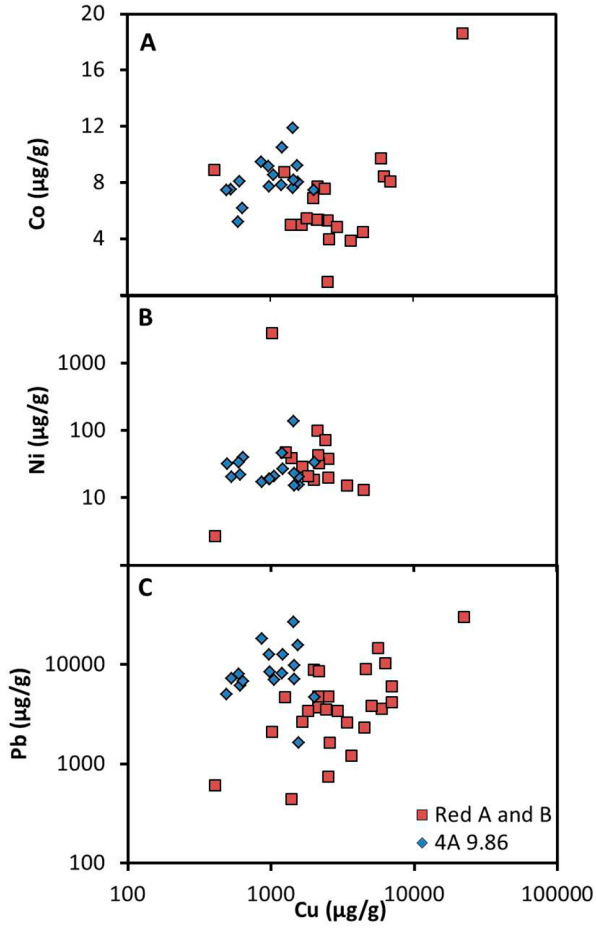

Figure 5. Log-scale covariate diagrams exhibiting concentrations of Co (A), Ni (B), and Pb (C) against those for Cu in red Trinitite samples.

Trinitite are plotted in Figure 9A. Also, the Zn abundances for red Trinitite and for the two Cu samples (Bingham and Keweenaw) are compared to their respective Pb isotope ratios in Figure 9B.

DISCUSSION

The extremely high concentrations of both Pb and Cu within red areas of Trinitite clearly indicate that both metals are of anthropogenic origin. Therefore, the red areas of Trinitite can be used to fingerprint the Pb isotope signature of the anthropogenic Pb used in the device and origin of the industrial Cu employed within it. Consequently, the Pb isotope ratios for the *in situ* analyses recording the highest concentrations of Pb (n = 5, >12,000 μg/g; see theSupporting Information) were used to constrain the signature of the anthropogenic Pb (Figure 6). Hence, the best estimate for the Pb isotope composition of the latter ($^{206}Pb/^{204}Pb$ = 17.86–17.96, $^{207}Pb/^{204}Pb$ = 15.53–15.60, and $^{208}Pb/^{204}Pb$ = 37.76–37.95) is much better constrained than previously reported (Figure 6).[3] The new Pb isotope data reported here indicates that the Pb used in the device was likely sourced from Buchans Mine, Newfoundland, Canada (see the Supporting Information).[3,10] American Smelting and Refining Company owned the mine starting in 1928 and mining operations continued until 1984, so this timeline agrees with our interpretation. Also, several other mines are characterized by similar Pb isotope ratios as the anthropogenic Pb signature reported here, but

DOI: 10.1021/acs.analchem.5b00696
Anal. Chem. 2015, 87, 5380–5386

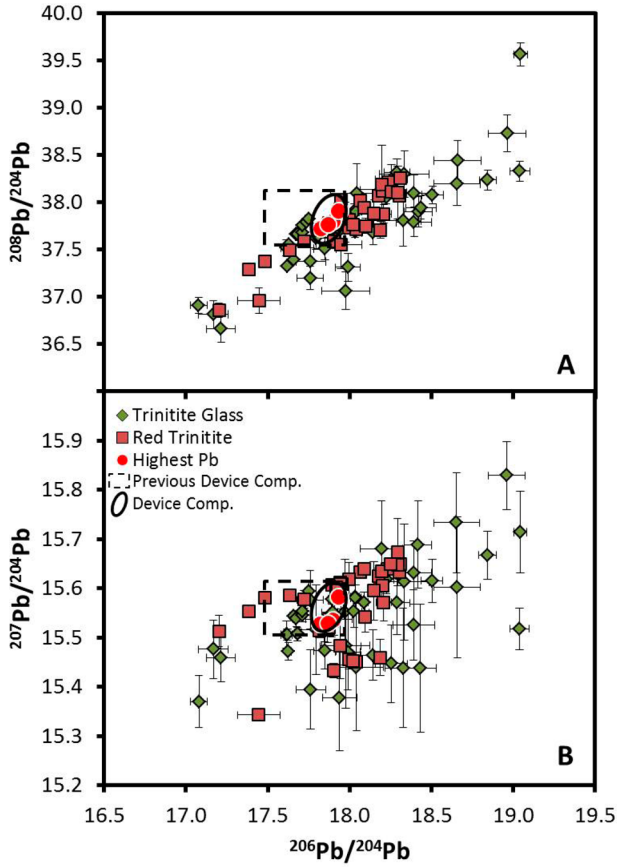

Figure 6. Pb−Pb isotope diagrams that show compositions of Trinitite glass,[3] red Trinitite, highest Pb concentration analyses (>15,000 μg/g), and the estimated Pb composition of the industrial Pb within the device. Previous estimated compositional field for the latter is also displayed.[3] Error bars at the 2σ level.

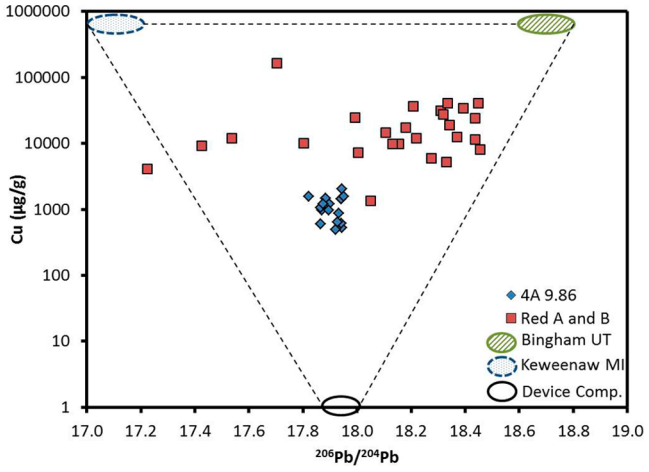

Figure 7. Cu concentrations (log scale) and corresponding Pb isotope ratios for the red Trinitite samples. Fields for industrial Cu samples (Bingham and Keweenaw) are plotted along with the estimated Pb isotope composition of industrial Pb employed within the device.

these mines were not active during that time period and are therefore not plausible candidates.[3,10] Although it is not documented where the industrial Pb in the device was employed, it may have been present in the shielding bricks, solder, or be used in another anthropogenic component.[3,8,23]

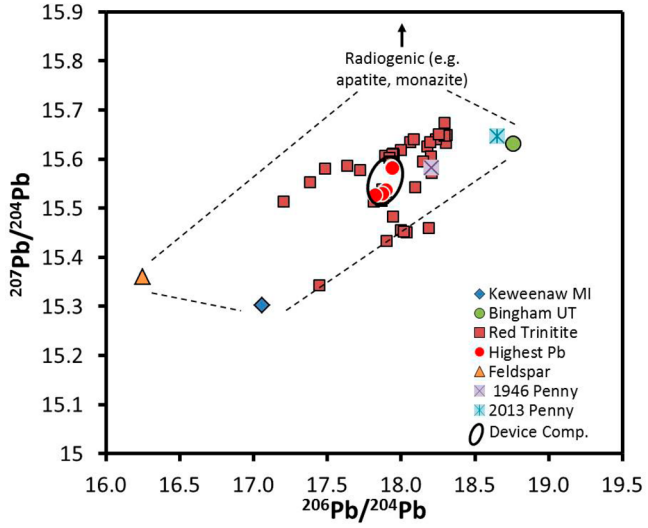

Figure 8. Pb−Pb isotope diagrams exhibiting analyses of red Trinitite, Cu samples (Bingham, UT, Keweenaw, MI, and 1946 and 2013 pennies), and a pristine feldspar grain.[3]

The elevated abundances of Cu present within Trinitite are attributed to the use of Cu wiring employed in the device/components because there is a lack of significant Cu-bearing minerals in the natural sand at ground zero.[7,8] In an attempt to determine the source of the anthropogenic (industrial) Cu present within the red inclusions of Trinitite, samples of manufactured Cu were investigated for their trace element and Pb isotopic compositions (see the Supporting Information). Of the samples investigated, two originate from mines that were active both before and during the Trinity Test: Bingham Mine, UT and the Keweenaw Peninsula, MI. A US penny produced in 1946 was also investigated since it is theorized that the US manufacturing industry would use the same source of industrial Cu to produce these items during the same time period as the Trinity test (i.e., 1940s). Lastly, a penny manufactured in 2013 was also investigated for comparative purposes. Figures 7 and 8 display the Pb isotope ratios for all Cu samples reported here, including the red Trinitite analyses. Figure 7 plots the Cu concentrations vs their corresponding Pb isotope ratios for the red Trinitite samples investigated here, and these plot within a triangular area defined by the Cu samples from Keweenaw and Bingham (assume ~100% Cu abundance for both) and the estimated anthropogenic Pb used in the device (assume ~0% Cu). Thus, the combined Cu abundances and associated Pb isotope ratios may be attributed to the mixing of the three components outlined in Figure 7. It is highly unlikely that each of the two single analyses reported here from both Cu ore deposits respectively represent the entire possible range of Pb isotope compositions for each mine. Especially since the formation of either native Cu deposits (Keweenaw, MI) or porphyry Cu sulfide ores (Bingham, UT) involve hydrothermal processes and scavenging of Cu and associated metals from the surrounding crustal rocks.[12,24] Thus, the relatively large difference between the Pb isotope compositions for the two deposits is the far more important factor, and these are consistent with their age of formation; i.e., the older Proterozoic (~1000 Ma) native Cu deposit at Keweenaw[11,12,16] is characterized by a less radiogenic Pb isotope composition compared to that for the much younger (~34 Ma) Bingham[24,25] porphyry Cu ore. Therefore, the Pb isotope

DOI: 10.1021/acs.analchem.5b00696
Anal. Chem. 2015, 87, 5380−5386

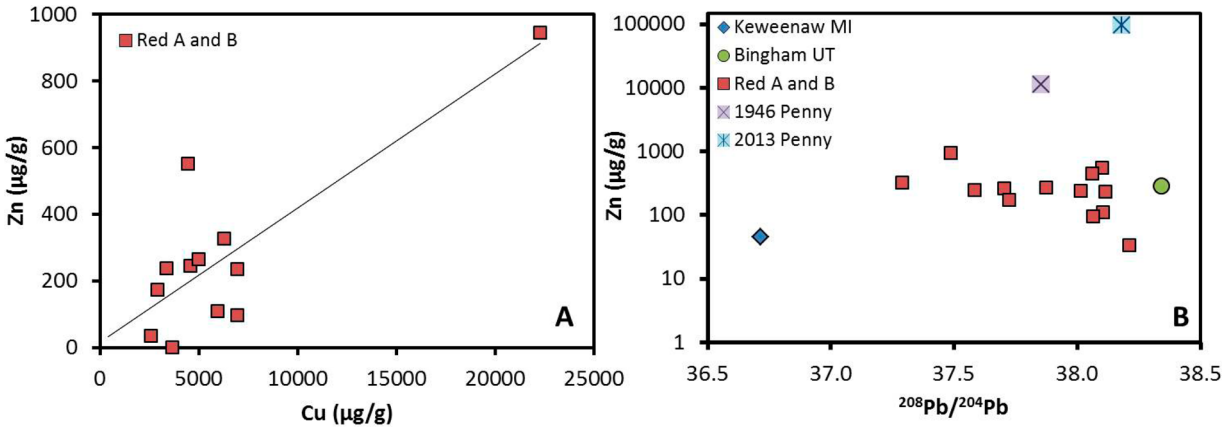

Figure 9. A) Zn and Cu concentrations in Red A and B Trinitite samples. B) Pb isotope ratios of red Trinitite and Cu samples vs Zn concentrations (μg/g; log scale).

compositions for both Cu deposits would ideally be represented each by fields rather than a single point (Figure 7). Figure 8 demonstrates that the total variation in Pb isotope ratios defined by red Trinitite may be attributed to the input of Pb from 4 distinct sources: from both Michigan's Upper Peninsula (UP) and Utah regions, as well as urano- and thorogenic minerals (e.g., zircon, apatite, monazite) and U- and Th-free minerals (e.g., K-feldspar) found in the natural sand.

Of interest, the Pb isotope composition for the 1946 penny plots proximal to that for the Trinity device, whereas that for the 2013 penny falls very close to the Bingham Cu sample (Figure 8). Production of the two pennies is separated by a period of 67 years, and their Pb isotope ratios suggest a significant drop in the input of Cu ore from the UP region of Michigan over time relative to the production of the US penny; a feature that is corroborated by the absence of Cu mining within the UP region today. Moreover, the metal composition of the US penny has changed dramatically over the years since it now consists predominantly of Zn.[26]

Zinc concentrations within red Trinitite samples Red A and B range between 100 and 900 μg/g and are significantly higher than the ~70 μg/g abundance of Zn in the natural sand of the blast area (Figure 9A, see the Supporting Information).[22] The concentrations of Cu and Zn within samples Red A and B delineate a general positive correlation (Figure 9A), which may be attributed to the presence of Zn in the Cu produced from the Bingham mine (Figure 9B). The Zn abundances of red Trinitite and for the two Cu samples (Bingham and Keweenaw) are also compared to their respective Pb isotope ratios (Figure 9B). The Cu nugget from Keweenaw is characterized by a relatively low Zn concentration of ~50 μg/g, whereas the Cu sample from Bingham has a much higher abundance of Zn (~300 μg/g). The combined Zn concentrations and Pb isotope ratios for red Trinitite plot in-between those for the two Cu samples (Figure 9) and is (at the very least) consistent with the interpretation that the Cu wiring used in the device likely derived from a mixture of Cu produced from mines within the UP and Bingham deposits.

CONCLUSIONS

Red inclusions within Trinitite contain extremely high abundances of Pb and Cu when compared to the natural sand at ground zero indicating that these metals are of anthropogenic origin and derived from the Trinity device and associated infrastructure. Hence, the red areas were used to accurately determine the Pb isotope signature of the anthropogenic Pb employed within the device, and these correspond to industrial Pb ore originating from the Buchans Mine, Newfoundland (Canada). This mine was owned and operated by an American company during the time of the Trinity test. The Pb isotope and trace element compositions of red Trinitite (Cu-rich) areas indicate that the industrial Cu contained within the device's wiring was likely a mix between two major producers of industrial Cu (Bingham, UT and Keweenaw, MI) prior to the time of the Trinity test and the Manhattan Project. The ability to determine the industrial source of metals found within postdetonation materials is of utmost importance, because these can provide insightful clues as to the fabrication and origin of the nuclear device, which will ultimately aid in source attribution.

ASSOCIATED CONTENT

Supporting Information

Additional information noted as Supporting Information in the text. The Supporting Information is available free of charge on the ACS Publications website at DOI: 10.1021/acs.analchem.5b00696.

AUTHOR INFORMATION

Corresponding Author

*Phone: 574-631-5380. E-mail: ekoeman@nd.edu.

Author Contributions

The manuscript was written through contributions of all authors. All authors have given approval to the final version of the manuscript.

Notes

The authors declare no competing financial interest.

ACKNOWLEDGMENTS

This work is funded by DOE/NNSA Grant PDP11-40/DE-NA0001112. We thank Sandy Dillard, Brazos Valley Petrographic Thin Section Services Lab (Bryan, TX) for production of quality thin sections. We also thank Dr. Ian Steele for his guidance with electron microprobe analysis. Constructive comments provided by two anonymous reviewers are greatly appreciated.

DOI: 10.1021/acs.analchem.5b00696
Anal. Chem. 2015, 87, 5380−5386

REFERENCES

(1) Fahey, A. J.; Zeissler, C. J.; Newbury, D. E.; Davis, J.; Lindstrom, R. M. *Proc. Natl. Acad. Sci. U. S. A.* **2010**, *107*, 20207−20212.
(2) Bellucci, J. J.; Simonetti, A.; Wallace, C.; Koeman, E. C.; Burns, P. *Anal. Chem.* **2013**, *85*, 4194−4198.
(3) Bellucci, J. J.; Simonetti, A.; Wallace, C.; Koeman, E. C.; Burns, P. *Anal. Chem.* **2013**, *85*, 7588−7593.
(4) Parekh, P.; Semkow, T.; Torres, M.; Haines, D.; Cooper, J.; Rosenberg, P.; Kitto, M. J. *Environ. Radioact.* **2006**, *85*, 103−120.
(5) Belloni, F.; Himbert, J.; Marzocchi, O.; Romanello, V. *J. Environ. Radioact.* **2011**, *102*, 852−862.
(6) Ross, C. S. *Am. Mineral.* **1948**, *33*, 360−362.
(7) Eby, N.; Hermes, R.; Charnley, N.; Smoliga, J. A. *Geol. Today* **2010**, *26* (5), 180−185.
(8) Eby, N.; Charnley, N.; Pirrie, D.; Hermes, R.; Smoliga, J.; Rollinson, G. *Am. Mineral.* **2015**, *100*, 427−441.
(9) Bellucci, J. J.; Simonetti, A. *J. Radioanal. Nucl. Chem.* **2012**, *293*, 313−319.
(10) Sangster, D.; Outridge, P.; Davis, W. *Environ. Rev.* **2000**, *8* (2), 115−147.
(11) Rapp, G., Jr.; Allert, J.; Vitali, V.; Jing, Z.; Henrickson, E. *Determining geologic sources of artifact copper: Source characterization using trace element patterns*; University Press of America: Lanham, MD, 2000.
(12) Rapp, G., Jr.; Henrickson, E.; Allert, J. Native copper sources of artifact copper in pre-Columbian North America. In *Archaeological geology of North America*; Lasca, N. P., Donahue, J., Eds.; Geological Society of America: Boulder, CO, 1990; Centennial Special, Vol. *4*, pp 479−498.
(13) Mauk, J. L.; Hancock, R. G. V. *Archaeometry* **1998**, *40* (1), 97−107.
(14) Cooper, H. K.; Duke, M. J. M.; Simonetti, A.; Chen, G. *J. Archaeol. Sci.* **2008**, *35*, 1732−1747.
(15) Simonetti, A.; Gariepy, C.; Banic, C. M.; Tanabe, R.; Wong, H. K. *Geochim. Cosmochim. Acta* **2004**, *68* (16), 3285−3294.
(16) Bornhorst, T. J.; Barron, R. J. Copper deposits of the western Upper Peninsula of Michigan. In *Archean to Anthropocene: Field Guides to the Geology of the Mid-Continent of North America*; Miller, J. D., Hudak, G. J., Wittkop, C., McLaughlin, P. I., Eds.; The Geological Society of America: Field Guide, 2011; Vol. *24*, pp 83−99.
(17) James, L. P. *Econ. Geol.* **1978**, *73*, 1218−1227.
(18) Jenner, G. A.; Longerich, H. P.; Jackson, S. E.; Freyer, B. J. *Chem. Geol.* **1990**, *83*, 133−148.
(19) Chen, W.; Simonetti, A. *Chem. Geol.* **2013**, *353*, 151−172.
(20) Baker, J.; Peate, D.; Waight, T.; Meyzen, C. *Chem. Geol.* **2004**, *211*, 275−303.
(21) Manhès, G.; Minster, J. F.; Allegre, C. J. *Earth Planet. Sci. Lett.* **1978**, *39*, 14−24.
(22) Bellucci, J. J.; Simonetti, A.; Koeman, E. C.; Wallace, C.; Burns, P. C. *Chem. Geol.* **2014**, *365*, 68−86.
(23) Rhodes, R. *The Making of the Atomic Bomb*, 1st ed.; Simon and Schuster: New York, 1986; pp 575−577, 657.
(24) Stacy, J. S.; Moore, W. J.; Rubright, R. D. *Earth Planet. Sci. Lett.* **1967**, *2*, 489−499.
(25) Keith, J. D.; Whitney, J. A.; Hattori, K.; Ballantyne, G. H.; Christiansen, E. H.; Barr, D. L.; Cannon, T. M.; Hook, C. J. *J. Petrol.* **1997**, *38* (12), 1679−1690.
(26) Mathur, R.; Titley, S.; Hart, G.; Wilson, M.; Davignon, M.; Zlatos, C. *J. Archaeol. Sci.* **2009**, *36*, 430−433.

DOI: 10.1021/acs.analchem.5b00696
Anal. Chem. 2015, 87, 5380−5386